Topology of the ground state of two interacting Bose-Einstein condensates

Francesco Riboli* and Michele Modugno†
INFM-LENS, Dipartimento di Fisica, Università di Firenze, Via Nello Carrara 1, 50019 Sesto Fiorentino, Italy
(Received 20 February 2002; published 13 June 2002)

We investigate the spatial patterns of the ground state of two interacting Bose-Einstein condensates. We consider the general case of two different atomic species (with different mass and in different hyperfine states) trapped in a magnetic potential whose eigenaxes can be tilted with respect to the vertical direction, giving rise to a nontrivial gravitational sag. Despite the complicated geometry, we show that within the Thomas-Fermi approximations and upon appropriate coordinate transformations, the equations for the density distributions can be put into a very simple form. Starting from these expressions we give explicit rules to classify the different spatial topologies that can be produced, and we discuss how the behavior of the system is influenced by the interatomic scattering length. We also compare explicit examples with the full numeric Gross-Pitaevskii calculation.

DOI: 10.1103/PhysRevA.65.063614 PACS number(s): 03.75.Fi, 05.30.Jp

I. INTRODUCTION

Bose-Einstein condensation of mixtures of different atomic species has recently been the subject of an intensive experimental and theoretical research [1–12]. The first experimental realization of a system of two interacting Bose-Einstein condensates (BECs) has been obtained at JILA with a double condensate of ^{87}Rb in two different hyperfine states, $|F,M_F\rangle=|1,-1\rangle$ and $|2,2\rangle$ [1]. This mixture was characterized by a partial overlap between the two condensates, in the presence of a gravitational ''sag'' due to the different magnetic moment. Since then several other experiments have been performed with double condensates of rubidium [2–4] and with spinor condensates of sodium in optical traps [5].

Motivated by these experiments and by the future possibility of realizing other binary mixtures of interacting BECs, these systems have been extensively studied also from the theoretical point of view. Up to now only two particular cases have been addressed: (i) a system of two condensates with different mass in cylindrically symmetric potentials arranged concentrically [6,7,10,11], and (ii) including a gravitational sag, but for condensates with the same mass (the JILA case) [12].

In this paper we extend these studies by considering the very general case of two different atomic species, with different mass and in different hyperfine states, trapped in a magnetic potential whose eigenaxes can be tilted with respect to the direction of gravity. We show that, despite the complicated geometry, the ground state of the system can be easily characterized within the Thomas-Fermi (TF) approximation valid for large numbers of atoms. We provide general formulas that allow us to calculate the shape and the density distributions of the two BECs. Our results can be a useful tool to analyze future experiments.

The paper is organized as follows. In Sec. II we discuss the equations for the ground state of the system and show that upon an appropriate coordinate transformation, they can be put into a very simple spherical form. In Sec. III we discuss the general features of the model, and we give an explicit algorithm to classify all the different topologies that can be constructed by varying the number of atoms and the interatomic scattering length. We also work out some examples for the case of ^{87}Rb and ^{41}K, which is a promising system for the realization of a new binary mixture of BECs [15,16]. Finally we compare the results against the numerical solution of the full Gross-Pitaevskii (GP) equations for the system, finding a good agreement.

II. THE MODEL

Let us consider a system of two Bose-Einstein condensates with mass m_i and in the hyperfine state (F_i,M_{Fi}), each containing N_i atoms $(i=1,2)$, confined in a magnetic trap. The ground state of the system can be obtained by solving two coupled Gross-Pitaevskii equations for the condensate wave functions ψ_i [13],

$$\left[-\frac{\hbar^2}{2m_1}\nabla^2+U_1(\mathbf{x})+u_{11}|\psi_1|^2+u_{12}|\psi_2|^2\right]\psi_1=\mu_1\psi_1, \tag{1}$$

$$\left[-\frac{\hbar^2}{2m_2}\nabla^2+U_2(\mathbf{x})+u_{21}|\psi_1|^2+u_{22}|\psi_2|^2\right]\psi_2=\mu_2\psi_2, \tag{2}$$

with the normalization condition

$$\int d^3x|\psi_i|^2=N_i. \tag{3}$$

The coupling constants u_{ij} are given in terms of the scattering length a_{ij} by [12]

$$u_{11}=\frac{4\pi\hbar^2a_{11}}{m_1}, \tag{4}$$

*Electronic address: riboli@lens.unifi.it
†Electronic address: modugno@fi.infn.it

$$u_{12}=2\pi\hbar^2 a_{12}\left(\frac{m_1+m_2}{m_1 m_2}\right)=u_{21}, \tag{5}$$

$$u_{22}=\frac{4\pi\hbar^2 a_{22}}{m_2}, \tag{6}$$

where we used the fact that $a_{12}=a_{21}$. Hereinafter we assume a_{11}, $a_{22}>0$.

The total potential experienced by each condensate is the sum of the gravitational potential and of a dipole magnetic potential $U_B^i(\mathbf{x})=\mu_B g_{Fi} M_{Fi}|B(\mathbf{x})|$ (g_{Fi} is the gyromagnetic factor of the specie i) which we assume, as usual, to be harmonic,

$$U_B^{(i)}(\mathbf{x})=\mu_B g_{Fi} M_{Fi}\left(B_0+\frac{1}{2}\sum_j K_j x_j^2\right). \tag{7}$$

By defining $\overline{K}=(K_1K_2K_3)^{1/3}$, $\lambda_j=\sqrt{K_j/\overline{K}}$, and

$$U_{0i}=\mu_B g_{Fi} M_{Fi} B_0, \tag{8}$$

$$\omega_i^2=\mu_B g_{Fi} M_{Fi}\overline{K}/m_i, \tag{9}$$

we can finally write U_B in the standard form

$$U_B^{(i)}(\mathbf{x})=\frac{1}{2}m_i\omega_i^2\sum_j \lambda_j^2 x_j^2+U_{0i}. \tag{10}$$

For what concerns the gravitational potential, here we consider the general case in which the vertical direction (the direction of gravity) is not aligned with any of the symmetry axis of the trap, but lies in the x-z symmetry plane, rotated by an angle θ. We include this possibility since in the experiments the trap confinement is generally weaker along the horizontal direction x, and therefore even a small angle can produce a large ''horizontal sag''; we will give explicit examples in the following section [14]. The total potential is

$$U_i(\mathbf{x})=U_B^{(i)}(\mathbf{x})+m_i g(x\sin\theta+z\cos\theta). \tag{11}$$

By performing an appropriate transformation on the coordinates the potential $U(\mathbf{x})$ can be put in a simpler form. These transformations amount to

(i) a scaling by λ_j (notice that the determinant of the transformation is equal to 1),

$$x_j\rightarrow x_j'\equiv\lambda_j x_j, \tag{12}$$

in order to put $U_B(\mathbf{x}')$ in a spherically symmetric form;

(ii) a rotation of an angle φ ($x_j'\rightarrow x_j''$) in order to align the z'' axis with the vertical direction,

$$\varphi=\tan^{-1}\left(\frac{\lambda_z}{\lambda_x}\tan\theta\right). \tag{13}$$

The transformed potential reads (to simplify the notations in the following we omit the apices, $x_j''\rightarrow x_j$)

$$U_i(\mathbf{x})=\frac{1}{2}m_i\omega_i^2[r^2+(z-z_{0i})^2]+U_{0i}, \tag{14}$$

where we have defined $r^2=x^2+y^2$, and

$$U_{0i}=\mu_B g_{Fi} M_{Fi} B_0-\frac{1}{2}m_i\frac{g^2 l^2}{\omega_i^2}, \tag{15}$$

$$z_{0i}=-\frac{g l}{\omega_i^2}, \tag{16}$$

where the scaling factor l is given by

$$l=\frac{\cos\theta}{\lambda_z\cos\varphi}. \tag{17}$$

Then we perform a translation along z by z_{01}, defining $dz=z_{02}-z_{01}$, and we express all quantities in dimensionless units, rescaling lengths by $a_{ho}\equiv\sqrt{\hbar/(m\omega_1)}$ and energies by $\hbar\omega_1$. Finally, the expressions for the trapping potential that will be used in the rest of the paper are

$$V_1(\mathbf{x})\equiv U_1(\mathbf{x})-U_{01}=\frac{1}{2}(r^2+z^2), \tag{18}$$

$$V_2(\mathbf{x})\equiv U_2(\mathbf{x})-U_{02}=\frac{1}{2}\eta[r^2+(z-dz)^2], \tag{19}$$

with

$$\eta=\frac{m_2\omega_2^2}{m_1\omega_1^2}=\frac{g_{F2}M_{F2}}{g_{F1}M_{F1}}, \tag{20}$$

$$dz=\frac{lg}{a_{ho}}\left(\frac{1}{\omega_2^2}-\frac{1}{\omega_1^2}\right)=\frac{lg}{a_{ho}\omega_1^2}\left(\frac{m_2}{\eta m_1}-1\right). \tag{21}$$

To summarize, in this section we have shown that with suitable transformations the trapping potential for the two condensates can be reduced to a simple spherical form. This allows for a much easier investigation of the features of the interacting system, as will be discussed in the following section.

III. THOMAS-FERMI APPROXIMATION

For large numbers of atoms N_i the solution of Eqs. (1) and (2) can be derived in the so-called Thomas-Fermi approximation that amounts to neglecting the kinetic terms $\nabla^2\psi_i$. Therefore, by reabsorbing the values U_{0i} of the potentials on their minima in the definition of the chemical potentials, $\mu_i-U_{0i}\rightarrow\mu_i$, the above equations become

$$V_1(\mathbf{x})+u_{11}|\psi_1|^2+u_{12}|\psi_2|^2=\mu_1, \tag{22}$$

$$V_2(\mathbf{x})+u_{21}|\psi_1|^2+u_{22}|\psi_2|^2=\mu_2, \tag{23}$$

where the reduced coupling constants u_{ij} are

$$u_{11}=4\pi\frac{a_{11}}{a_{ho}}, \tag{24}$$

$$u_{12}=2\pi\frac{a_{12}}{a_{ho}}\left(1+\frac{m_1}{m_2}\right)=u_{21}, \tag{25}$$

$$u_{22}=4\pi\frac{a_{22}}{a_{ho}}\frac{m_1}{m_2}. \tag{26}$$

By defining $\gamma_1\equiv u_{21}/u_{11}$, $\gamma_2\equiv u_{12}/u_{22}$, and $\Delta=u_{11}u_{22}-u_{12}^2$, the solution of Eqs. (22) and (23) in the overlapping region take the form

$$|\psi_1|^2=\alpha_1[R_1^2-r^2-(z-z_{c1})^2], \tag{27}$$

$$|\psi_2|^2=\alpha_2[R_2^2-r^2-(z-z_{c2})^2], \tag{28}$$

where we have defined the radii R_i,

$$R_1^2(\mu_1,\mu_2)=\frac{2(\mu_1-\gamma_2\mu_2)}{1-\eta\gamma_2}+\frac{\eta\gamma_2}{(1-\eta\gamma_2)^2}dz^2, \tag{29}$$

$$R_2^2(\mu_1,\mu_2)=\frac{2(\mu_2-\gamma_1\mu_1)}{\eta-\gamma_1}+\frac{\eta\gamma_1}{(\eta-\gamma_1)^2}dz^2; \tag{30}$$

the position of the centers along z,

$$z_{c1}=\frac{-\eta\gamma_2}{1-\eta\gamma_2}dz, \tag{31}$$

$$z_{c2}=\frac{\eta}{\eta-\gamma_1}dz; \tag{32}$$

and the normalization factors α_i,

$$\alpha_1=u_{22}\frac{1-\eta\gamma_2}{2\Delta}, \tag{33}$$

$$\alpha_2=u_{11}\frac{\eta-\gamma_1}{2\Delta}. \tag{34}$$

Notice that in order to have overlap between ψ_1 and ψ_2 Eqs. (27) and (28) both have to be satisfied, that is, both right members must be positive ($|\psi_1|^2,|\psi_2|^2\geqslant 0$). The overlapping region between the two condensates is therefore the intersection of the regions of space delimited by the spherical surfaces Σ_i defined by the equation $R_i^2=r^2+(z-z_{ci})^2$, and identified by the sign of the coefficient α_i: for $\alpha_i>0$ the region to be considered is the one inside the surface Σ_i, for $\alpha_i<0$ the one outside.

In the regions where there is not an overlap the wave functions take the usual form

$$|\psi_{01}|^2=\frac{1}{2u_{11}}(2\mu_1-r^2-z^2), \tag{35}$$

$$|\psi_{02}|^2=\frac{\eta}{2u_{22}}\left(\frac{\mu_2}{\eta}-r^2-(z-dz)^2\right). \tag{36}$$

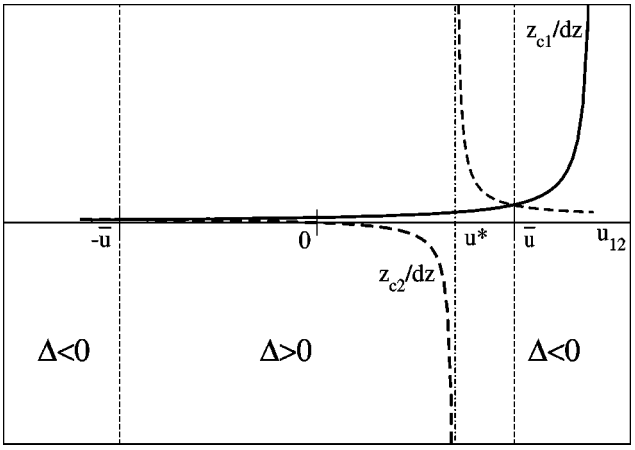

FIG. 1. Plot of the rescaled position z_{c1}/dz (continuous line) and z_{c2}/dz (dashed line) of the centers of the ''interacting'' surfaces Σ_i as a function of the mutual coupling u_{12}.

Analogously to the overlapping case, these solutions are defined in a region of space whose boundary is delimited by the surfaces Σ_{0i} of equation $R_{0i}^2=r^2+(z-z_{ci}^0)^2$, with $R_{01}^2=2\mu_1$, $R_{02}^2=2\mu_2/\eta$, $z_{c1}^0=0$, and $z_{c2}^0=dz$.

Notice that in order to satisfy the continuity condition of the wave function ψ_i at the interface between the overlapping and nonoverlapping regions the wave function ψ_{01} must be connected to ψ_1 at the boundary defined by Σ_2 (where $|\psi_2|^2$ vanishes, but not $|\psi_1|^2$), and vice versa.

A. General considerations

Even though a self-consistent solution of the full problem can be obtained only after having imposed the normalization of the wave functions, we can draw some general considerations by considering the role played by the determinant Δ and the coupling u_{12}. First of all we define the value of u_{12} at which the determinant Δ changes sign, $\bar{u}\equiv\sqrt{u_{11}u_{22}}$. Then we notice that the behavior of the position of the centers along z, z_{ci}, and the normalization factors α_i of the overlapping wave functions depend on two critical values $u_{12}=\eta u_{11}$ and $u_{12}=u_{22}/\eta$, which define the poles of z_{ci} and the zeros of α_i (the latter have poles also for $u_{12}=\pm\bar{u}$. It is not difficult to prove that one of these two values lies in the interval where $\Delta>0$, and the other outside. Therefore, to fix the hierarchy of the scattering lengths we choose the condensate 1 in order to satisfy the condition $\eta^2\leqslant u_{22}/u_{11}$; with this choice the critical value lying in the interval of positive Δ is $u^*\equiv\eta u_{11}$. In Figs. 1 and 2 we show the position of the centers z_{ci} and the normalization factors α_i as a function of u_{12}. Notice that in correspondence of u^* the center z_{c2} of the surface Σ_2 goes from $-\infty$ to $+\infty$, and the normalization factor α_2 becomes negative. Therefore for $u^*<u_{12}<\bar{u}$ the region where $|\psi_2|^2>0$ is the one outside the surface Σ_2 [see also Figs. 3(c) and 3(g)].

We can distinguish three cases:

(i) $u_{12}<-\bar{u}$, $\Delta<0$: no overlapping solution is allowed in this range. From Fig. 2 we see that both α_i are negative, and therefore it is not difficult to prove that an overlapping re-

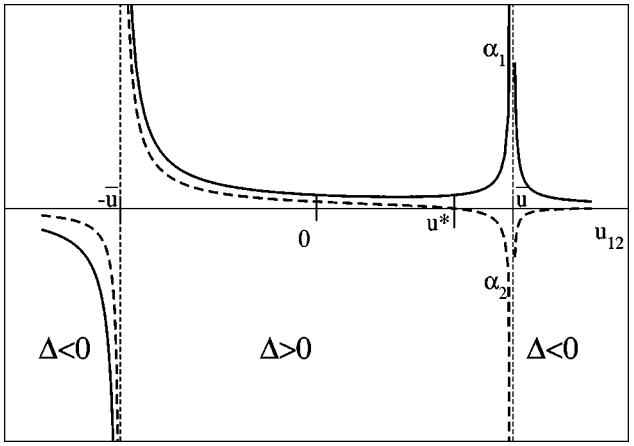

FIG. 2. Plot of the normalization factors α_1 (continuous line) and α_2 (dashed line) of the interacting wave functions as a function of u_{12} (in arbitrary units).

gion could be constructed only at the price of putting a hole in the condensate, where both ψ_i would be vanishing. This has obviously no physical meaning and in fact what actually happens is that when u_{12} approaches $-\bar{u}^+$ the condensates eventually collapse [7,12].

(ii) $-\bar{u}<u_{12}<\bar{u}$, $\Delta>0$: in this range the two condensates can coexist and overlap in some region of space if $|dz|<R_{10}+R_{20}$. We will discuss in detail the actual degree of overlap and its topology in the following section.

(iii) $u_{12}>\bar{u}$, $\Delta<0$: in this case the strong mutual repulsion leads to a phase separation between the two condensates [8,9]. The actual shape of the interface is determined by the one at the critical value $\bar{u}$. Since for this value the overlap goes to zero (in the TF approximation), if one further increases u_{12} the shape of the interface cannot change.

Of course, if one retains the kinetic term in the GP equations this can in part affect the degree of overlap between the two condensates. In particular the transition to the phase-separation regime is not so sharp: the condensates can have an appreciable overlap also for $u_{12}\gtrsim\bar{u}$ [10–12]. The effect of the kinetic energy is also to raise the critical value below which the system collapses.

B. Topology of spatial configurations

In this section we investigate the different configurations that can be obtained in the case (ii) discussed above ($\Delta>0$, $-\bar{u}<u_{12}<\bar{u}$). Before solving completely the system for some particular set of parameters, we give an overview of the different topologies that one can obtain. We again distinguish three cases, as shown in Fig. 3.

(1) ''External overlap'': this case can take place when the separation $|dz|$ between the centers is larger than the difference of the radii of the noninteracting profiles, $|R_{01}-R_{02}|<|dz|<R_{01}+R_{02}$ [see Figs. 3(a)–3(d)]. One can easily verify that all the four surfaces Σ_1 and Σ_{01} intersect on a circle perpendicular to the plane in Fig. 3, passing for the points P and Q (shown as black dots). The overlapping region is the one contained between the surfaces Σ_1 and Σ_2

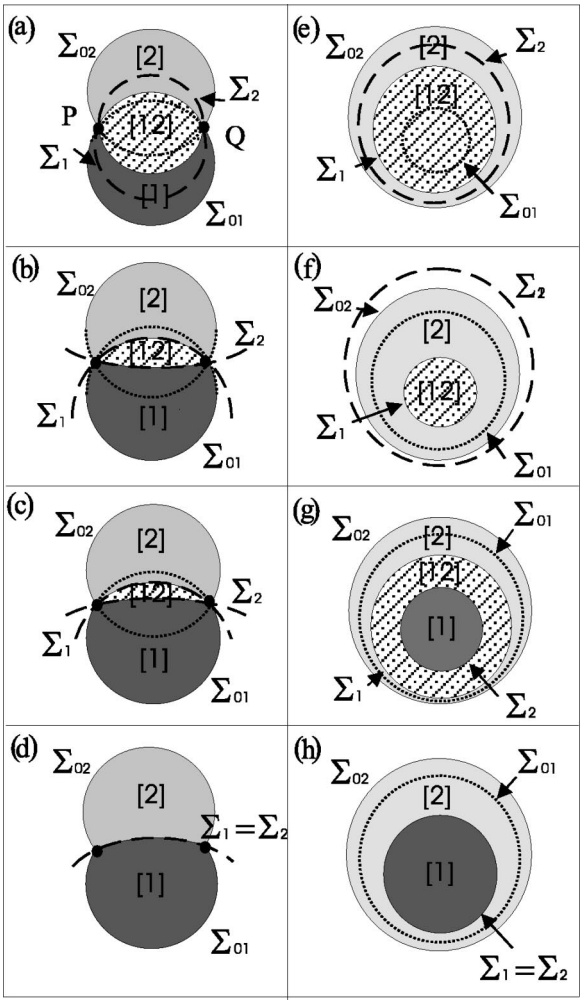

FIG. 3. Possible topologies for a binary mixture of two BECs. (1) ''External overlap'': $u_{12}<0$ (a), $0<u_{12}<u^*$ (b), $u^*<u_{12}<\bar{u}$ (c), and phase separation $u_{12}=\bar{u}$ (d); (2) ''full overlap'': $u_{12}<0$ (e), $0<u_{12}<u^*$ (f); (3) ''partial overlap'': $u^*<u_{12}<\bar{u}$ (g) and phase separation $u_{12}=\bar{u}$ (h). Dark and light gray represent the regions occupied by the noninteracting condensates 1 and 2, respectively. The shaded area indicates the overlapping region. The boundaries of these regions are delimited by the surfaces Σ_{0i} (noninteracting, continuous, and dotted lines) and Σ_i (overlapping, dashed lines).

(dashed lines in the figure) whose actual shape depends on u_{12}, as shown in Fig. 3 for $u_{12}<0$ (a), $0<u_{12}<u^*$ (b), $u^*<u_{12}<\bar{u}$ (c), and $u_{12}=\bar{u}$ which is a case of phase separation (d). For smaller dz one obtains other configurations, which fall into the next two classes.

(2) ''Full overlap'': in this case, for $|dz|<|R_{01}-R_{02}|$, one of the two condensates is entirely contained in the other with whom it is fully overlapping. See Figs. 3(e) and 3(f) for $u_{12}<0$ and $0<u_{12}<u^*$, respectively. Which of the two condensates lies in the outer shell depends on the actual value of the parameters [6].

(3) ''Partial overlap'': this is similar to case (2), but now the mutual repulsion between the two condensates is great enough to expel each from the central region of the other and force the overlap to occur only at the boundary between

them. In particular, with the choice $\eta u_{11} \leqslant \overline{u}$, the overlap takes place over a shell that separates the inner core containing the condensate 1, and the outer region with the condensate 2 [Fig. 3(g)]. Notice that according to the above discussion this configuration is possible only for $u^* < u_{12} < \overline{u}$ where the sign of α_2 is negative. This is a necessary but not sufficient condition, since also the condition $R_2 < R_1$ must be satisfied. In this range of u_{12} (where $\alpha_2 < 0$) another possible solution is $R_2^2 < 0$, which leads to the case (2). By further increasing u_{12} to the critical value $\overline{u}$ one again obtains a configuration of phase separation [Fig. 3(h)].

Having determined the possible configurations of the system, we are now ready to solve any particular problem by imposing the normalization condition (3). To do this one has to write the normalization integrals for each of the possible profiles in Fig. 3, and then solve Eq. (3) in order to find the chemical potentials μ_i as a function of the atom numbers N_i. The analytic expressions for these integrals are given in the Appendix. These are polynomial functions of fractional powers in the chemical potentials μ_i, and in general Eq. (3) does not admit analytical solutions. Therefore the relation between μ_i and N_i must be inverted numerically (which is nevertheless a much easier task than solving numerically the full Gross-Pitaevskii problem). For the special case of phase separation the two normalization equations can be decoupled (by using the fact that $R_1 = R_2$ and $z_{c1} = z_{c2}$ for $u_{12} = \overline{u}$), and solved analytically for $dz = 0$.

Notice that in general (except for some particular case, e.g., $dz = 0$) it is not possible to know *a priori* which of the various configurations in Fig. 3 applies: one has to solve Eq. (3) for all the possible configurations, and then choose the one that gives a self-consistent solution.

In summary the ground-state configuration for a particular system can be found in three steps:

(i) Choose the normalization integrals that apply to the possible profiles in Fig. 3 for a given u_{12}, and determine $\mu_i(N_i)$ by solving Eq. (3) self-consistently;

(ii) identify the overlapping region by plotting the ''interacting'' surfaces Σ_i;

(iii) determine the noninteracting region for each condensate by using the ''noninteracting'' surfaces Σ_{0i}, and the continuity of the wave functions (see Fig. 3).

We also recall that for the very special case $dz = 0$ there are also symmetry-breaking solutions, not included in the present analysis, which could be energetically favorable [10].

C. Examples

To show how the method works we now give some explicit examples by considering two condensates of ^{87}Rb and ^{41}K, which is a promising system for the realization of a new binary mixture of BECs [15,16]. We will classify some possible configurations that can be obtained by varying the trap parameters and the number of atoms in each condensate, for different values of the interatomic scattering length, which is considered here as a tunable parameter [18]. The specific values will be chosen in order to generate configurations for all the three classes discussed in the preceding section. The results, valid in the TF approximation, will be compared with the numeric solution of the full three-dimensional Gross-Pitaevskii equations (GPE), found using a steepest descent method [13].

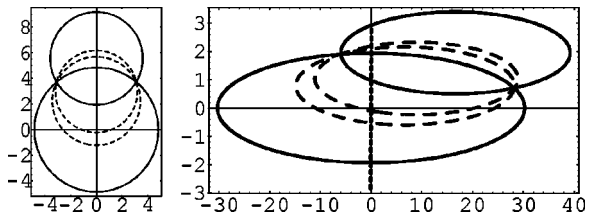

FIG. 4. TF profiles of the two condensates (noninteracting, continuous; overlapping, dashed) in rescaled (left) and natural (right, in units of a_{ho}) coordinates (x horizontal, z vertical) for a case of ''external overlap'': $N_{\mathrm{Rb}} = 5 \times 10^4$, $N_{\mathrm{K}} = 2 \times 10^4$, $a_{12} = -55\ a_0$.

We start by considering a case of ''external overlap'' with both condensates in the hyperfine level $|2,2\rangle$ ($\eta = 1$). The scattering lengths are $a_{\mathrm{Rb}} = 99\ a_0$ and $a_{\mathrm{K}} = 60\ a_0$, a_0 being the Bohr radius [17]. As trap frequencies we use $\omega_x^{\mathrm{Rb}} = 16$ Hz, $\omega_y^{\mathrm{Rb}} = \omega_z^{\mathrm{Rb}} = 250$ Hz, with an angle of rotation $\theta = 0.035$ (we retain these values for all the cases analyzed in this section). With this choice the reduced coupling constant u_{ii} are

$$u_{\mathrm{Rb,Rb}} = 0.0611, \quad u_{K,K} = 0.0785, \tag{37}$$

and therefore, according to the above discussion, we identify the condensates 1 with ^{87}Rb, and the condensates 2 with

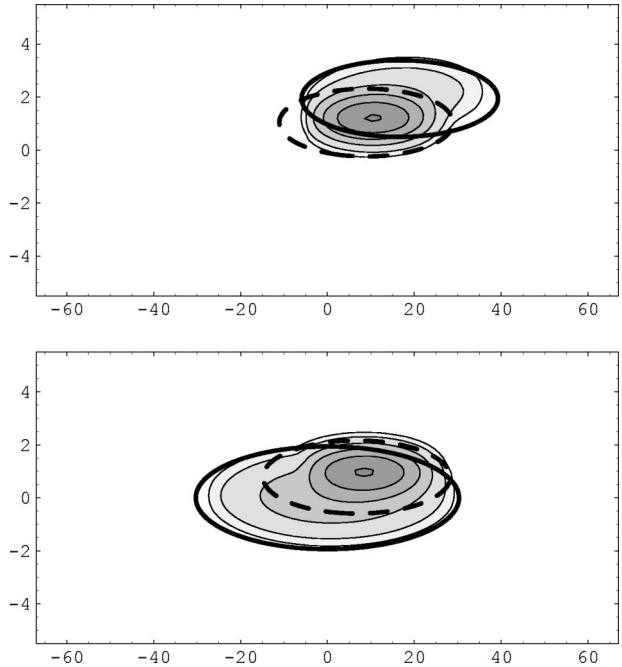

FIG. 5. Density contours of the GPE solutions in the x-z plane for the ^{87}Rb (bottom) and ^{41}K (top) condensates. Each condensate is compared with the TF profiles that define the boundary of the noninteracting or overlapping phases, as defined in Fig. 3(a). This is a case of ''external overlap'' with attractive interaction between the two condensates, $a_{12} = -55\ a_0$, and $N_{\mathrm{Rb}} = 5 \times 10^4$, $N_{\mathrm{K}} = 2 \times 10^4$. Lengths are given in units of a_{ho}.

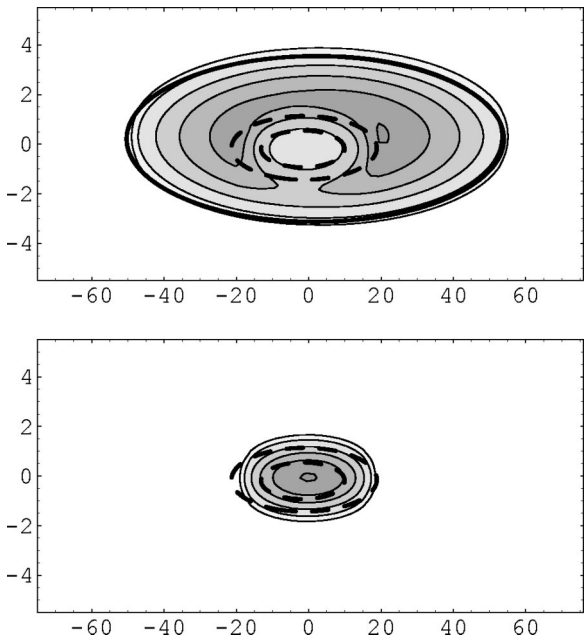

FIG. 6. Density contours of the GPE solutions in the x-z plane for the ^{87}Rb (bottom) and ^{41}K (top) condensates, for a case of ''partial overlap'': $N_{\mathrm{Rb}}=2\times10^4$, $N_{\mathrm{K}}=2\times10^5$, $a_{12}=67\ a_0$. Each condensate is compared with the TF profiles which define the boundary of the noninteracting or overlapping phases, as defined in Fig. 3(g). Lengths are given in units of a_{ho}.

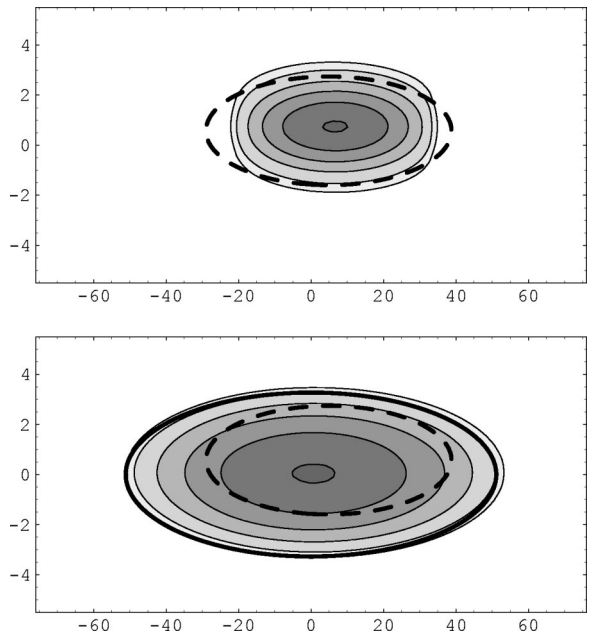

FIG. 7. Density contours of the GPE solutions in the x-z plane for the ^{87}Rb (bottom) and ^{41}K (top) condensates, for a case of ''full overlap'': $N_{\mathrm{Rb}}=5\times10^5$, $N_{\mathrm{K}}=1\times10^4$, $a_{12}=20\ a_0$. Each condensate is compared with the TF profiles which define the boundary of the noninteracting or overlapping phases, as defined in Fig. 3(f). Lengths are given in units of a_{ho}.

^{41}K. We choose a case of attractive interaction between the two condensates, $a_{12}=-55\ a_0$ ($u_{12}=-0.0530$), with $N_{\mathrm{Rb}}=5\times10^4$ and $N_{\mathrm{K}}=2\times10^4$. To visualize the role of the scaling and rotation transformations, in Fig. 4 we show the TF profiles of the two condensates in the x-z plane, in rescaled (left) and natural coordinates (the coordinate axes correspond to the trap eigenaxes; right). The profiles in natural units can be easily obtained by performing the inverse transformation of those in Eqs. (12) and (13). We will use this system of coordinates to show all the following figures. Notice that despite the small rotation angle θ, (the direction of gravity, represented by a dotted line in the right picture of Fig. 4, is almost indistinguishable from the z axis on the scale of the figure) the misalignment in the direction of gravity produces a relatively large horizontal sag in the x direction where the trap confinement is weak.

In Fig. 5 we compare the TF profiles with the contour plot of the two densities, as found from the full GPE solution. For clarity each condensate is plotted separately, and compared with the TF profiles that define the boundary of the noninteracting (continuous lines) or overlapping phases (dashed lines), as defined in Fig. 3. The outer contour line for each condensate correspond to 10% of its peak density (for $y=0$).

Then we consider two examples for a system where the ^{87}Rb condensate is in the hyperfine level $|2,2\rangle$ and the ^{41}K condensate in $|2,1\rangle$ (we use again $a_{\mathrm{K,K}}=60\ a_0$). In this case $\eta=0.5$. In Fig. 6 we show a case of ''partial overlap,'' obtained by fixing the interatomic scattering length to $a_{12}=67\ a_0$ ($u_{12}=0.0645$) and the number of atoms to $N_{\mathrm{Rb}}=2\times10^4$ and $N_{\mathrm{K}}=2\times10^5$. Notice that when both condensates are in the $|2,2\rangle$ level the spatial separation between the two is too large to allow for a configuration of ''partial overlap'' for reasonable values of the trap frequencies (in principle, one could reduce the separation by strongly increasing the confinement in the direction of gravity).

Finally, in Fig. 7 we show a case of ''full overlap'' for $N_{\mathrm{Rb}}=5\times10^5$, $N_{\mathrm{K}}=1\times10^4$, and $a_{12}=20\ a_0$, giving $u_{12}=0.0193$.

From the examples considered here we see that, although the full solution of the GPE is required for a precise determination of the actual degree of overlap between the two condensates, the TF approximation well captures the basic topology of the ground-state configurations. Therefore, due to its simplicity, the TF method presented here can be a useful tool to characterize the ground-state structure of a binary mixture of BECs also in presence of a nontrivial geometry.

We conclude this section by noting that we have also verified that our method well reproduces the results already studied in literature in case of simpler geometries [6,10,12].

IV. CONCLUSIONS

We have presented a general method to classify the ground state of a binary mixture of Bose-Einstein condensates. We have considered the general case of two different atomic species, with different mass and in different hyperfine states, trapped in a magnetic potential. We have explicitly included the possibility of a nontrivial gravitational sag, when the direction of gravity is not aligned with any of the trap eigenaxes, since even a small misalignment can produce

a large ''horizontal sag.'' We have shown that, within the Thomas-Fermi approximations and by performing a suitable coordinate transformation, the equations for the density distributions can be put into a simple spherical form. We have given explicit rules to classify the different spatial topologies that can be produced, and we have discussed how the behavior of the system is influenced by the interatomic interaction.

We have also provided explicit examples, and compared the results with the full numeric Gross-Pitaevskii calculation, finding a good agreement.

The results presented in this paper might be useful for analyzing future experiments where new combinations of binary condensates are likely to be produced [15,16].

Note added. After completing this work, we became aware of a very recent preprint related to this subject [19].

ACKNOWLEDGMENTS

We acknowledge useful discussion with G. Modugno and G. Roati.

APPENDIX: NORMALIZATION INTEGRALS

In this appendix we give the explicit expressions for the integrals that enter the normalization condition (3). We distinguish two general cases: (i) ''internal overlap,'' one of the two condensates is entirely contained in the other (Fig. 3, right column), and (ii) ''external overlap'' (Fig. 3, left column).

In both cases the normalization condition can be written as a sum of integrals of a generic density

$$|\psi|^2=\alpha[R_c^2-r^2-(z-z_c)^2] \tag{A1}$$

over an appropriate portion of spherical domain whose boundary is given by the surface

$$R_A^2=r^2+(z-z_A)^2. \tag{A2}$$

In the following sections we consider explicitly the two cases.

1. Internal overlap

In this case the normalization condition can be imposed by using a combination of integrals over *spherical* domains. The generic form is

$$I_I(\alpha,z_c,R_c,z_A,R_A)=4\pi\alpha R_A^3\left[\frac{1}{3}R_c^2-\frac{1}{3}(z_c-z_A)^2-\frac{1}{5}R_A^2\right]. \tag{A3}$$

From this expression one can also recover the value of the integral for the noninteracting case

$$I_n(\mu_i)=\frac{8\pi}{15}\alpha R_c^5 \tag{A4}$$

$[I_n(\mu_i)=4\pi(2\mu_i)^{5/2}/u_{ii}$ for $\eta=1]$.

By using appropriate combinations of the integral (A3), the normalization condition for the case shown in Fig. 3(g) reads

$$\begin{aligned}N_1=&I_I[\alpha_1,z_{c1},R_1(\mu_1,\mu_2),z_{c1},R_1(\mu_1,\mu_2)]\\&-I_I[\alpha_1,z_{c1},R_1(\mu_1,\mu_2),z_{c2},R_2(\mu_1,\mu_2)]\\&+I_I[\alpha_{01},0,\sqrt{2\mu_1/\eta},z_{c2},R_2(\mu_1,\mu_2)],\end{aligned} \tag{A5}$$

$$\begin{aligned}N_2=&I_n(\mu_2)-I_I[\alpha_{02},dz,\sqrt{2\mu_2/\eta},z_{c1},R_1(\mu_1,\mu_2)\\&+I_I(\alpha_2,z_{c2},R_2(\mu_1,\mu_2),z_{c1},R_1(\mu_1,\mu_2)]\\&-I_I[\alpha_2,z_{c2},R_2(\mu_1,\mu_2),z_{c2},R_2(\mu_1,\mu_2)],\end{aligned} \tag{A6}$$

where we have indicated the explicit dependence on μ_1 and μ_2. The cases in Figs. 3(e), 3(f), and 3(h) can be constructed in a similar way.

2. External overlap

These are the configurations shown in Fig. 3(a)–(d). In this case the master integral can be written as the integral over a *convex* domain delimited by two spherical surfaces (A and B the upper and lower ones along the z axis, respectively)

$$\begin{aligned}&I_E(\alpha,z_c,R_c,z_A,R_A,z_B,R_B)\\&=\pi\alpha\{R_A^2[R_c^2-0.5R_A^2-(z_c-z_A)^2][R_A-\overline{z}(A,B)]\\&\quad-R_A^2(z_c-z_A)[R_A^2-\overline{z^2}(A,B)]-\tfrac{1}{3}[R_c^2-(z_c-z_A)^2]\\&\quad\times[R_A^3-\overline{z^3}(A,B)]+\tfrac{1}{2}(z_c-z_A)[R_A^4-\overline{z^4}(A,B)]\\&\quad+\tfrac{1}{10}[R_A^5-\overline{z^5}(A,B)]\}+(z_A\leftrightarrow z_B,R_A\leftrightarrow -R_B)\end{aligned} \tag{A7}$$

with

$$\overline{z}(A,B)=\frac{R_A^2-R_B^2+(z_B-z_A)^2}{2(z_A-z_B)}. \tag{A8}$$

By assuming a configuration where the condensate 1 has a lower position along z (as in Fig. 3), the normalization condition for the cases with $u_{12}<u^*$ shown in Figs. 3(a) and 3(b) is

$$\begin{aligned}N_1=&I_n(\mu_1)-I_E[\alpha_{01},0,\sqrt{2\mu_1},0,\sqrt{2\mu_1},z_{c2},R_2(\mu_1,\mu_2)]\\&+I_E[\alpha_1,z_{c1},R_1(\mu_1,\mu_2),z_{c1},R_1(\mu_1,\mu_2),z_{c2},R_2\\&\times(\mu_1,\mu_2)],\end{aligned} \tag{A9}$$

$$\begin{aligned}N_2=&I_n(\mu_2)\\&-I_E(\alpha_{02},dz,\sqrt{2\mu_2/\eta},z_{c1},R_1(\mu_1,\mu_2),dz,\sqrt{2\mu_1})\\&+I_E[\alpha_2,z_{c2},R_2(\mu_1,\mu_2),z_{c1},R_1(\mu_1,\mu_2),z_{c2},R_2\\&\times(\mu_1,\mu_2)].\end{aligned} \tag{A10}$$

In an analogous way one can construct the appropriate normalization condition for all other cases in this class (''external overlap''), by considering the appropriate combination of integrals of the form (A7) over *convex* domains.

[1] C.J. Myatt, E.A. Burt, R.W. Ghrist, E.A. Cornell, and C.E. Wieman, Phys. Rev. Lett. **78**, 586 (1997).

[2] D.S. Hall, M.R. Matthews, J.R. Ensher, C.E. Wieman, and E.A. Cornell, Phys. Rev. Lett. **81**, 1539 (1998); D.S. Hall, M.R. Matthews, C.E. Wieman, and E.A. Cornell, *ibid.* **81**, 1543 (1998).

[3] J.L. Martin, C.R. McKenzie, N.R. Thomas, J.C. Sharpe, D.M. Warrington, P.J. Manson, W.J. Sandle, and A.C. Wilson, J. Phys. B **32**, 3065 (1999).

[4] P. Maddaloni, M. Modugno, C. Fort, F. Minardi, and M. Inguscio, Phys. Rev. Lett. **85**, 2413 (2000).

[5] D.M. Stamper-Kurn, M.R. Andrews, A.P. Chikkatur, S. Inouye, H.-J. Miesner, J. Stenger, and W. Ketterle, Phys. Rev. Lett. **80**, 2027 (1998); J. Stenger, S. Inouye, D.M. Stamper-Kurn, H.-J. Miesner, A.P. Chikkatur, and W. Ketterle, Nature (London) **396**, 345 (1998).

[6] Tin-Lun Ho and V.B. Shenoy, Phys. Rev. Lett. **77**, 3276 (1996).

[7] C.K. Law, H. Pu, N.P. Bigelow, and J.H. Eberly, Phys. Rev. Lett. **79**, 3105 (1997); H. Pu and N.P. Bigelow, *ibid.* **80**, 1130 (1998).

[8] E. Timmermans, Phys. Rev. Lett. **81**, 5718 (1998).

[9] P. Ao and S.T. Chui, Phys. Rev. A **58**, 4836 (1998).

[10] M. Trippenbach, K. Góral, K. Rzazevski, B. Malomed, and Y.B. Band, J. Phys. B **33**, 4017 (2000).

[11] R.A. Barankov, e-print cond-mat/0112326.

[12] B.D. Esry, C.H. Greene, J.P. Burke, and J.L. Bohn, Phys. Rev. Lett. **78**, 3594 (1997).

[13] F. Dalfovo, S. Giorgini, L.P. Pitaevskii, and S. Stringari, Rev. Mod. Phys. **71**, 463 (1999).

[14] In general one could consider the situation in which the vertical direction does not lie in any of symmetry planes of the trap. Anyway, since most experiments are performed with cylindrically symmetric traps, we restrict our analysis to this case. The extension to the case of anisotropic traps is straightforward.

[15] G. Modugno, G. Ferrari, G. Roati, R.J. Brecha, A. Simoni, and M. Inguscio, Science **294**, 1320 (2001).

[16] G. Ferrari, M. Inguscio, W. Jastrzebski, G. Modugno, G. Roati, and A. Simoni, e-print cond-mat/0202290.

[17] H. Wang *et al.*, Phys. Rev. A **62**, 052704 (2000); E.G.M. van Kempen, S.J.J.M.F. Kokkelmans, D.J. Heinzen, and B.J. Verhaar, Phys. Rev. Lett. **88**, 093201 (2002).

[18] Although the scattering length $a_{Rb,K}$ has been recently estimated to be of the order of 163 a_0 [16], in principle, it is possible to tune its value by using Feshbach resonances.

[19] D.M. Jezek and P. Capuzzi, e-print cond-mat/0202025.